Toward a Predictive Model of Hot Spring Water from Modern and Ancient Travertine Depositional Facies

John Veysey II[1], Thomas J. Schickel[2], Bruce W. Fouke[2], Mike Kandianis[2], Roy Johnson[2] and Nigel Goldenfeld[1]

1: University of Illinois Department of Physics

2: University of Illinois Department of Geology

ABSTRACT

Over a period of seven years we have collected an extensive data set of the physical, chemical, and microbiological attributes of two hot springs located in the Mammoth Hot Springs complex of Yellowstone National Park. We report a strong correlation between travertine depositional facies and the temperature, pH, and flux of hot spring water. Because advection dominates in these hot spring drainage systems, this correlation allows identification of controlling processes on a macroscopic scale. This provides a basis for the use of facies models to reconstruct modern and ancient carbonate aqueous environments. Within the context of the travertine facies, we construct a model to define the primary flow path, quantify variability between and within springs, and explain two previously reported trends in microbial community diversity.

Key Words:

Yellowstone National Park

Travertine Facies

Calcium carbonate hot springs

23 Microbial community diversity

24 Fluid transport modeling

INTRODUCTION

The concept of sedimentary depositional facies serves as a fundamental means for reconstructing aqueous paleoenvironments from the geological record (Flügel 2004; Wilson 1975). However this basic facies concept is broadly defined, contains many assumptions about the physics, chemistry, and biology of the environment, and spans multiple temporal and spatial scales. The classic definition of facies is based solely on specific characteristics of a body of sedimentary rock (Gressly 1838; Reading 1996). This original definition has been broadened and is now commonly used to describe the environmental processes *believed* to have formed the sedimentary deposit (Walker 1984). However, this secondary, interpretive sense of the word facies implicitly assumes knowledge of specific environmental conditions at the time of deposition. Yet despite the fundamental role of these assumptions, few studies have quantitatively examined the aqueous characteristics of modern depositional environments within a classic facies context. In this paper, we approach this problem by studying terrestrial hot springs, where deposition is so rapid that the connection between the modern facies and the aqueous environment can be readily made.

Most previous studies have included a combination of spring water chemistry, calcium carbonate geochemistry (Amundson and Kelly 1987; Folk et al. 1985; Ford and Pedley 1996; Friedman 1970; Herman and Lorah 1988; Lu et al. 2000; Pentecost 1990; Suarez 1983; Zhang et al. 2001), and controlled lab experiments that quantify precipitation dynamics (Busenberg and Plummer 1986; Dreybrodt et al. 1992; Kanakis and Dalas 2000; Liu and Dreybrodt 1997; Spanos and Koutsoukos 1998; Usdowski et

47 al. 1979; Van Cappellen et al. 1993). However, these investigations have generally not
48 simultaneously studied modern spring water, microbial communities, and solid $CaCO_3$
49 in a natural environment. Therefore, the results of these studies are not adequate for
50 comparing $CaCO_3$ precipitated in different hot springs (*travertine*) or reconstructing
51 paleoenvironments from ancient travertine.

52 In order to justify the environmental assumptions implicit in carbonate facies
53 models, our research at Mammoth Hot Springs has analyzed the depositional
54 environment within the context of a five-component facies model (Fouke et al. 2000).
55 We term these components the vent, apron channel, pond, proximal slope, and distal
56 slope facies. These five facies are not specific to Yellowstone hot springs; they have
57 been seen throughout the world (e.g., Rapolano Terme, in Tuscany, Italy (Fouke et al.
58 2001). In keeping with the original geological definition of facies (Reading 1996), our
59 model is based solely on the shape, structure, and chemistry of carbonate deposits on
60 the floor of the spring drainage system (Fouke et al. 2000).

61 Each facies includes unique travertine features on all length scales. For example,
62 on the scale of microns, the apron channel facies is comprised of aragonite needles
63 radiating from the outer walls of filamentous bacteria. But on the scale of centimeters to
64 meters, this facies is a 1-meter wide channel floored by streamer pavements (Fouke et
65 al. 2003; Fouke et al. 2000). Because different processes control carbonate precipitation
66 at each scale, we have analyzed the physical, chemical, and microbiological attributes
67 of the depositional environment within the following spatial hierarchy: (1)
68 “microscopic” on the scale of microns; (2) “mesoscopic” on the scale of millimeters to

centimeters; (3) “macroscopic” on a scale of meters to 10s of meters; and, (4) “system level” on the scale larger than 10s of meters. Each facies which we have defined incorporates the first 3 levels of spatial description, whereas the systems level scale includes all five facies.

Our previous investigations have examined microbial community structure and metabolic activities on length scales ranging from microns to 10s of meters (Fouke et al. 2003; Fouke et al. 2000). In addition, petrography has identified unique travertine features over the same length scales. Although aqueous and isotopic chemistry have suggested that CO_2 degassing is the dominant control on systems-level spring water evolution (Fouke et al. 2000; Fouke et al. 2001), petrography has demonstrated that microscopic processes can be expressed on a macroscopic scale. For example, in the apron channel facies, aragonite needle crystals encrust filamentous *Aquificales* bacteria (Fouke et al. 2003; Fouke et al. 2000), resulting in millimeter-wide travertine streamers that grow to meters in length. These travertine streamers aggregate to create the unique pavement which floors the entire apron channel.

In this paper we examine aqueous chemistry on the macroscopic scale and demonstrate that pH, temperature, and flux are sufficient to differentiate macroscopic patterns in calcium carbonate crystallization. We also define the concept of a primary flow path as means of connecting the macroscopic aqueous environment to smaller length scales. We quantify fluctuations in spring water pH, temperature, and flux, and demonstrate that these parameters are strongly correlated with the underlying depositional facies. Finally, we use our observations to explain two previously observed

91 trends in microbial diversity and community structure (Bonheyo et al. 2006; Fouke et
92 al. 2003). Our new results rigorously justify using facies models to characterize
93 depositional environments, and demonstrate that they may be used to reconstruct the
94 macroscopic chemical and physical properties of modern and ancient aqueous
95 environments.

96 **GEOLOGIC SETTING**

97 Mammoth Hot Springs, which lies on the northern flank of the Yellowstone
98 caldera, contains a succession of travertine deposits that range from 0 to approximately
99 8,000 years old that are 73 m in thickness and cover more than 4 km^2 (Allen and Day
100 1935; Bargar 1978; Sturchio et al. 1992; Sturchio et al. 1994; White et al. 1975). The
101 springs expel Ca-Na-HCO_3-SO_4 type hot waters derived from a subsurface reservoir at
102 temperatures of greater than 100^oC (Kharaka et al. 1991; Sorey 1991). Angel Terrace,
103 near the top of the Mammoth complex, contains several active small springs. We have
104 focused on two of these, AT-1 and AT-3, which are shown in Figure 1. The hydrologic
105 system is dynamic, with multiple vents appearing, sealing, and reopening on Angel
106 Terrace at a frequency of months to tens of years (Bargar 1978; Sorey 1991).

107 CHARACTERIZATION OF SPRING WATER

108 Correlation of the solid-phase travertine facies with the spring water has
109 required quantification of physical and chemical aqueous parameters within a complex,
110 heterogeneous natural environment that exhibits large spatial variations and temporal
111 fluctuations. Over a period of 7 years, our research group has collected measurements,

112 summarized in Table 1, of the physical, chemical, and biological properties of 2 hot
113 springs (AT-1 and AT-3) at Angel Terrace.

114 The springs were surveyed using a Brunton compass, a 30 m steel tape measure,
115 and a Garmin Model 12 GPS unit. The locations of all sample sites were determined
116 with respect to the vent. During each trip, samples were collected along *transects*,
117 defined as groups of measurements taken at nearly the same time at locations beginning
118 with the vent and proceeding downstream through the drainage system. All
119 measurements were taken in triplicate; the mean is taken as our best estimate of the true
120 value, and the standard deviation quantifies measurement accuracy.

121 343 pH measurements were taken *in situ*, using three types of temperature
122 correcting hand held probes: a Hach sensION 156 meter; an Orion Model 290A probe;
123 and an Oaktron Waterproof Series 300 meter. Different meters were needed because the
124 spring environment rapidly degrades and destroys probes. The meters were calibrated
125 before, during, and after each transect using standard pH buffer solutions (4.0, 7.0, and
126 10.0) with an accuracy of ±0.01 pH at 25^{o}C. pH measurements were complicated
127 because of the rapid deposition of $CaCO_3$ on the probe's electrode. In order to avoid
128 instrument drift and slow convergence to a steady measurement, the probes were
129 regularly steeped in a 0.1*M* HCl solution, rinsed in de-ionized water, and then
130 recalibrated.

131 Measurements of water temperature were taken at the same times and locations as pH
132 measurements, using the same probes. Temperature was also collected every 30 seconds
133 *in situ* using two Hobo Temperature Data loggers (Model H20-001).

Total flux in spring AT-3 was determined at the vent source using a propeller based current meter, USGS Pygmy Meter Model 6205, and by measuring the area through which current was flowing. We obtained an independent measure of flux on the January 2005 trip (Table 1) using time of flight techniques inside a channel which had a fixed cross sectional area. This method records the length of time over which small, floating travertine flakes need to travel a given distance. The pygmy meter was also used to characterize typical flow velocities in the spring system and, where possible, Pitot tubes were used to validate these measurements.

DEFINITION OF THE *PRIMARY FLOW PATH*

To connect macroscopic processes to those which control precipitation at a microscopic scale, we must follow the evolution of spring water as it progresses along a single *flow path*. A flow path is the set of points traversed by a packet of water as it moves from the vent to the distal slope. In a hot spring, unlike in a stream or river, water spreads out over a broad area; streams divide and recombine. The physical and chemical properties of water at a given point can depend in a complicated way on any number of upstream points, each of which could have different physical and chemical properties.

This problem can be resolved by defining the *primary flow path*. Given a contiguous area covered by spring water, the primary flow path is the set of points at a given distance from the vent which are traversed by the largest volume of water. Where a large percentage of the spring water follows along a single trajectory, the chemical and physical properties at a point are overwhelmingly related to those of its upstream

neighbor. This idea can be extended, and secondary or tertiary flow paths can be defined in regions of the spring which are disconnected by dry areas. This definition does not uniquely define a flow path in the sense of a streamline. When water spreads out evenly across an area, the primary flow path defined here can include a set of equivalent points.

While the primary flow path can sometimes be identified by visual inspection, this is not always the case, particularly in thin sheet flow further away from the vent. In this situation the primary flow path locally follows the trajectory along which temperature decreases most slowly as a function of distance.

In most carbonate hot springs there is only a single vent, and the temperature of spring water monotonically decreases after it leaves the vent. Until it equilibrates with the atmosphere, the temperature of a packet of water is only a function of the length of time since it emerged from the vent. If $\bar{}$ denotes temperature and $\cdot$ denotes time, then $\bar{}$. Consider the contour of all points which are the same distance, $|\overrightarrow{\ }|$, from the last identified point on the flow path, which we denote $\bar{}$. If we are looking nearby, $|\bar{}|$ must be small, and all these points will have the same water depth, H. In most of our system, this is a good approximation even for non-infinitesimal $|\overrightarrow{\ }|$. If $\overrightarrow{\ }$ is the local velocity, and $\Delta\vec{s}$ a small displacement along the equidistant contour, then flux $Q(\vec{r}_0 + \Delta\vec{r})$ at each of these points may be estimated as follows:

$$Q(\vec{r}_0 + \Delta\vec{r}) = H\Delta\vec{s}\,v(\vec{r}_0 + \Delta\vec{r}) \propto v(\vec{r}_0 + \Delta\vec{r}) \approx \frac{\Delta\vec{r}}{\Delta t} \qquad (1)$$

Here Δt denotes the time it takes a packet of water to go from $\vec{r}_0$ to $\vec{r}_0 + \Delta\vec{r}$. Because the points being considered are equidistant, $Q(\vec{r}_0 + \Delta\vec{r}) \propto \frac{1}{\Delta t}$. . If | | is sufficiently small, must also be small, and by expanding $f(t)$ for small , we can write . This implies that:

(2) Hence will be maximized where is minimized. The next point on the primary flow path will be the spot among these equidistant points with the smallest , or equivalently the spot with the highest temperature.

Thus we have shown that the primary flow path **locally** follows the trajectory along which temperature decreases most slowly as a function of distance. This theoretical discussion was applied to the data collected at spring AT-3 in 2004, and the primary flow path was determined by looking at the average temperatures at the 24 sample locations. The results in Figure 2 show that the points which comprise the primary flow path minimize , as we step from point to point. It locally minimizes the slope of the dotted line in Figure 4.Thus we have shown that the primary flow path locally follows the trajectory along which temperature decreases most slowly as a function of distance. This analysis provides a useful recipe for analyzing aqueous measurements and for organizing experiments at hot springs. If one proceeds downstream with a meter stick and a thermometer, and draws arcs with the meter stick, the next point in the flow path will be the point along the arc with the highest

196 temperature. When combined with standard qualitative observations, this approach
197 allows sampling strategies which account for mixed flow paths, regardless of variations
198 in water depth, velocity, or changes in underlying topography.
199
200 VARIABILITY AND FLUCTUATIONS IN HOT SPRING WATER
201 Table 2 compares the ranges of observed spring water temperatures and pH, as a
202 function of facies, for multiple hot springs and times. There is consistent overlap
203 between measurements from the same facies at different springs (AT1 and AT3), but
204 there are also large variations within each facies. Although this variability does not
205 obscure the overall down flow trends, identifying meaningful differences that exist
206 between or within hot springs requires first quantifying the macroscopic fluctuations
207 and variations that occur within a single spring.
208 Three kinds of variability are relevant to carbonate precipitation. First, there are
209 temporal fluctuations on the time scale of our measurements (e.g. 10's of seconds). In
210 our error model, these fluctuations are treated as measurement errors. Second, there are
211 temporal fluctuations on the time scale of days, such as changes in spring discharge.
212 These are relevant for comparing different measurements, but not for understanding
213 travertine deposits thicker than a few millimeters. Finally, there are spatial variations on
214 macroscopic scale. There are also spatial differences on both the microscopic and
215 systems-level scale which are not relevant to the scope of this discussion.
216 Figure 3 shows these three kinds of variability for both temperature and pH as a
217 function of facies. We quantified temporal fluctuations by considering the ensemble of

218 measurements at a given point in space (taken over a period of three days), calculating
219 the standard deviation of that ensemble, and then averaging those deviations over each
220 facies. We quantified spatial variations by grouping all measurements collected within a
221 facies at a given time, and then calculating the standard deviation of that ensemble. This
222 was repeated for measurements taken at different times, and the results were averaged
223 over each facies.

224 While the measurement errors are small (approximately 0.03 pH units and 1^{o}C),
225 there are significant temporal fluctuations and spatial variations. These differences are
226 not driven by large changes in the source water, as the vent exhibits the smallest
227 changes. Both fluctuations and variations result from the interplay of myriad smaller
228 factors that include: changes in the flow patterns upstream from a point; diurnal
229 insolation; changes in total spring flux; and atmospheric conditions, particularly wind.
230 We observed wind driving water over the pond lips, dramatically changing the pH and
231 temperature of downstream points, particularly in areas of low flux.

232 During a period of three days a HOBO temperature data logger in the proximal
233 slope recorded a maximum change of 9^{o}C, with a standard deviation of 2^{o}C. These
234 measurements exhibit a clear diurnal signal, driven by differences in daytime and
235 nighttime air temperatures as large as 20^{o}C. The fluctuations seen in the HOBO data are
236 consistent with the results shown in Figure 3.

237 Total spring flux was considerably more difficult to measure than either
238 temperature or pH. In June 2004, using a pygmy current meter, we estimated Spring
239 AT-3 discharge at 59 L/s. In January 2005, using time of flight techniques, we

240 measured 12 L/s. Both measurements are accurate to within 10%. These numbers
241 indicate significant variation in total spring flux, which will result in changes in
242 downstream aqueous chemistry, temperature, and flux -- even if the source water
243 remains otherwise unchanged. Our flux measurements do not agree with the report of
244 (Sorey 1991), who reported the total discharge of **all** hot springs in the Mammoth
245 complex as 59.1±3 L/s. . Sorey's result was based on the assumption that approximately
246 10% of the total groundwater erupts through hot springs. This assumption may be
247 incorrect, but the observed large variations in flux make it difficult to confidently
248 estimate total discharge.
249 Figure 3 shows a noteworthy trend in spatial variability. The largest heterogeneities in
250 temperature and pH are seen in the pond facies, and the most homogeneous regions are
251 the vent and distal slope facies. This occurs because the spring system is essentially
252 held fixed at the beginning and the end of the primary flow path. At the vent, pH and
253 temperature are held constant by the steady influx of homogeneous source water, which
254 has relatively constant temperature and chemistry (Table 2). In the distal slope, CO_2
255 fugacity asymptotically nears what would be expected for spring water in equilibrium
256 with both the atmosphere and solid $CaCO_3$ in the substrate. This largely determines pH
257 and temperature in the distal slope. The temporal fluctuations in temperature mirror the
258 trend seen in spatial variations.
259 Significantly, this trend in spatial variability could explain why the greatest
260 bacterial diversity is seen in the pond facies (Bonheyo et al. 2006; Fouke et al. 2003).
261 Our results show that the pond facies offers the broadest array of mesoscopic

physiochemical conditions. As a result, it can support the greatest microbial diversity (Brock et al. 1999). Conversely, the most homogeneous environments, at the beginning and end of the primary flow path, have been shown to support the least diverse bacterial communities (Bonheyo et al. 2006).

RELATING THE ROCK RECORD TO THE DEPOSITIONAL ENVIRONMENT

Despite large variations and fluctuations in the aqueous environment, we see statistically significant correlations between physical and chemical attributes of spring water and underlying depositional facies. These correlations exist because macroscopic $CaCO_3$ mineral precipitation occurs on time scales of days to months, and the rock record inherently averages out more rapid fluctuations in the aqueous environment.

Figure 4 shows the distribution of all pH and temperature measurements arranged by facies. It illustrates that the vent, apron channel, and distal slope facies can be identified by considering pH and temperature jointly, implying that these facies are associated with distinct depositional environments. The transition from the vent to the apron channel facies is associated with the pH increasing beyond 6.6 while temperature is relatively unchanged. This suggests that this transition is controlled by CO_2 exsolution and the onset of carbonate precipitation.

The pond and proximal slope facies cannot be differentiated from each other on the basis of spring water temperature and pH. While petrography documents some similarity on a microscopic level (Fouke et al. 2003; Fouke et al. 2000), clear distinctions (such as travertine dams and a terraced architecture) emerge on a

284 macroscopic level. We therefore considered additional physical parameters to
285 understand how the same spring water can give rise to two distinct aggregate
286 morphologies. These two facies are differentiated by average fluid velocity.
287 Velocities in these thin sheet flows are difficult to measure, particularly because
288 techniques like particle image velocimetry could negatively impact the natural hot
289 spring environment. We have used several independent techniques, including the
290 pygmy current meter, Pitot tubes, and time of flight measurements. We observed
291 velocities less than 20 cm/s in the pond, but over 35 cm/s in the proximal slope. The
292 average velocities in these facies are a function of slope, total flux, fluid depth, and
293 facies area. Using our measurements of area, depth, and total flux, we calculate
294 velocities consistent with these experimental findings. These results imply that, if
295 other factors remain unchanged, ponds will form in flatter areas with lower flux and the
296 proximal slope facies will form on steeper underlying topographies with higher flux.
297 This is consistent with qualitative observations at the springs AT-1 and AT-3, and also
298 agrees with computational models of these hot spring systems (Goldenfeld et al. 2006).
299 As the spring landscape evolves, both flux and slope change as a result of travertine
300 deposition. This can result in a steep proximal slope ultimately becoming terraced
301 ponds.
302 These results imply that, if other factors remain unchanged, ponds will form in
303 flatter areas with lower flux and the proximal slope facies will form on steeper
304 underlying topographies with higher flux. This is consistent with qualitative

observations at the springs AT-1 and AT-3, and also agrees with computational models of these hot spring systems (Goldenfeld et al. 2006).

The observed macroscopic partitions in spring water explain previous observations (Bonheyo et al. 2006; Fouke et al. 2003) which showed that microbial communities are also partitioned according to facies. Because different microorganisms thrive in different niches, microbial community structure must be correlated with the partitions seen in the aqueous environment.

RECONSTRUCTING MODERN AND ANCIENT ENVIRONMENTS

The strong correlations between travertine facies and the macroscopic physical and chemical parameters of the depositional environment allow each facies to be uniquely identified solely by pH, temperature, and flow velocity. While fluctuations and variations complicate comparisons between springs, we have shown that when viewed statistically (Figure 4), measurements taken from the same facies in different springs are equivalent, as long as the facies have had sufficient time to establish themselves since the last major change in vent location or fluxOur qualitative observations at spring AT-2 suggest that facies need a few to establish themselves.

When combined with previous work (Bonheyo et al. 2006; Fouke et al. 2003; Fouke et al. 2000), these results demonstrate that these travertine depositing hot springs exhibit the same macroscopic partitions chemically, physically, petrographically, and microbially. The only other study which reports hot spring temperature and pH in the

context of aggregate morphology (Chafetz and Lawerance 1994) is consistent with the partitions shown in Figure 4. Note that cooler carbonate springs which have significantly different source water temperature will not develop the same five facies, and are therefore not comparable.

This simple linkage is a powerful predictive tool, implying that the facies model, which inherently averages fluctuations and variations, can be directly used for paleoenvironmental reconstructions. Our results also put precise quantitative bounds on the temperature and pH of the spring water from which ancient travertine facies originally precipitated. As an example, Folk and Chafetz (Folk et al. 1985) documented streamers in Pleistocene travertine, primary crystallization features which were preserved despite subsequent post-depositional physical and chemical alterations (diagenesis, Bathurst 1975)Their description suggests that these deposits were formed in the apron channel facies. Utilizing Figure 4, we conclude that these deposits precipitated from spring waters with a pH of 6.75 ± 0.13 and a temperature of 65.5 ± 3.7 ^{o}C.

CONCLUSIONS

During six trips spanning seven years, we collected a large, comprehensive set of measurements which characterize the spring water, travertine, and microbial ecology at two carbonate hot springs in Yellowstone National Park. Although the aqueous

environment of these springs exhibits large spatial variations and temporal fluctuations on the macroscopic scale, we have shown that pH, temperature, and flux are sufficient to tie the spring water to the underlying depositional facies. The observed strong correlations between travertine facies and the spring water remove any assumptions about the aqueous environment during deposition. This validates the facies concept as a macroscopic framework for comparing modern hot springs. These results allow us to put more accurate quantitative bounds on paleoenvironmental reconstructions from ancient travertine. A subsequent paper will address in detail how microscopic aqueous chemistry and the kinetics of travertine nucleation and crystallization give rise to the correlations documented here. In this sense, the present study is a necessary first step toward a fundamental predictive model of travertine precipitation in hot springs.

361 ACKNOWLEDGEMENTS

362 This work was supported by research awards from the NSF Biocomplexity in the
363 Environment Program (EAR 0221743), the ACS PRF Starter Grant Program (34549-
364 G2), and the UIUC Critical Research Initiative. The conclusions of this study are those
365 of the authors, and do not necessarily reflect those of the funding agencies. Thanks to G.
366 Bonheyo, D. Fike, B. Sansenbacher, H. Garcia Martin, K. Hutchings for assistance with
367 data collection. We also thank A. Murray, A. Kameda, and B. Carter for field work,
368 helpful comments and HOBO temperature data. We are indebted to the National Park
369 Service, particularly B. Suderman, H. Hessler, and C. Hendrix, for their support,
370 assistance, passion, and ongoing preservation of Yellowstone hot springs.

371 FIGURES

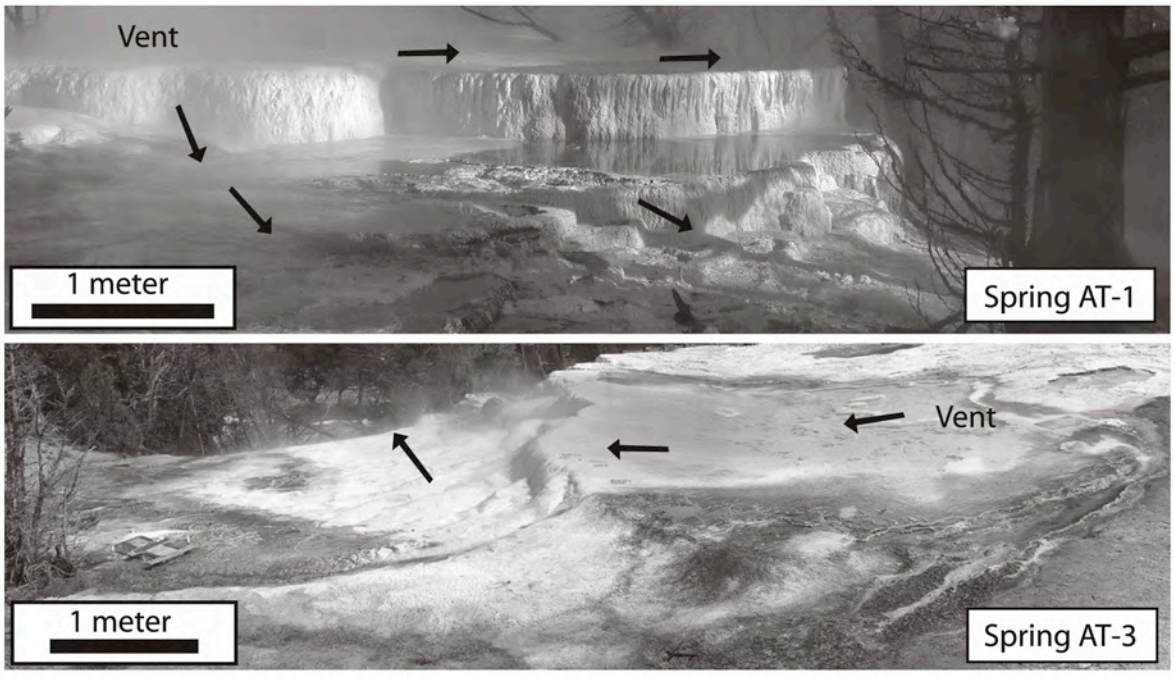

372

373 Figure 1. Spring AT-1 and AT-3 showing vent and general direction of spring water

374 flow.

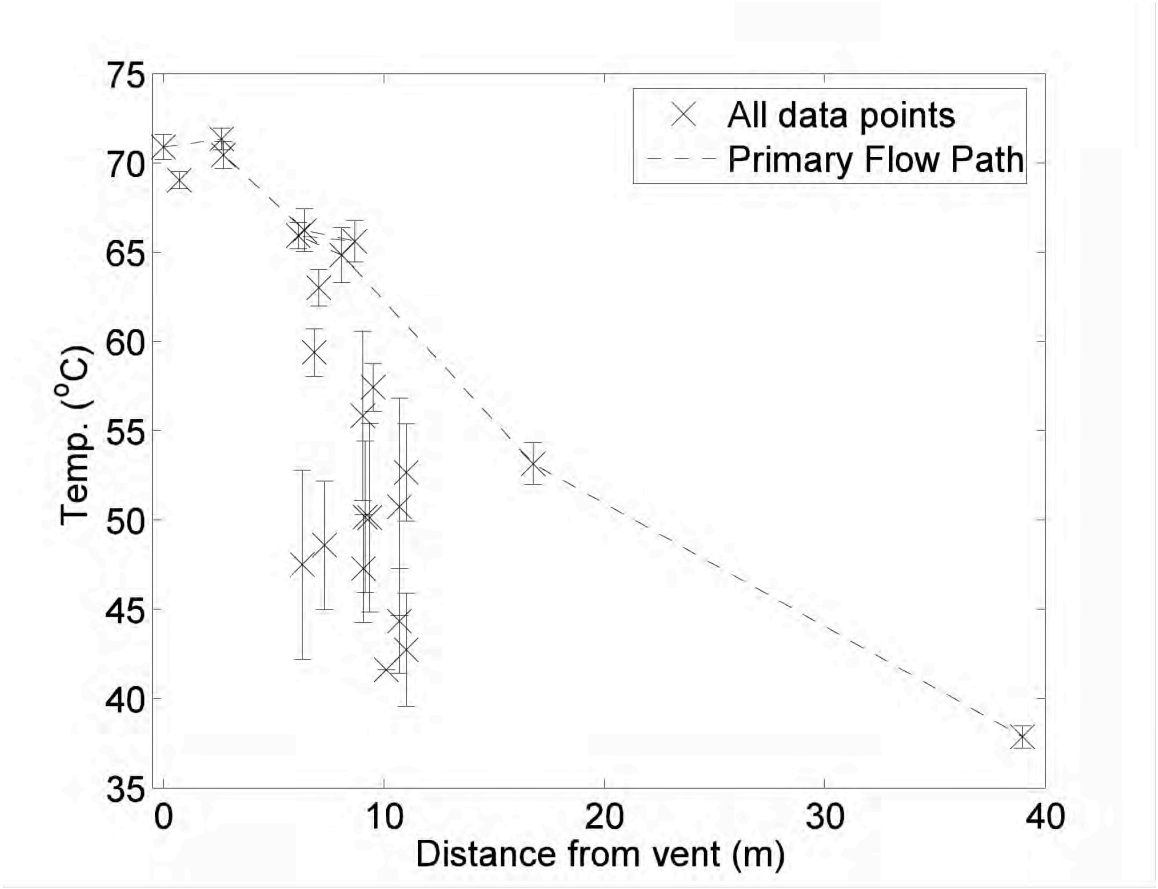

375

376 Figure 2. pH and temperature values observed at Spring AT-3 during 2004. Each point
377 represents the average of 5 triplicate measurements at each of 24 sample locations,
378 taken over a period of 3 days.

379

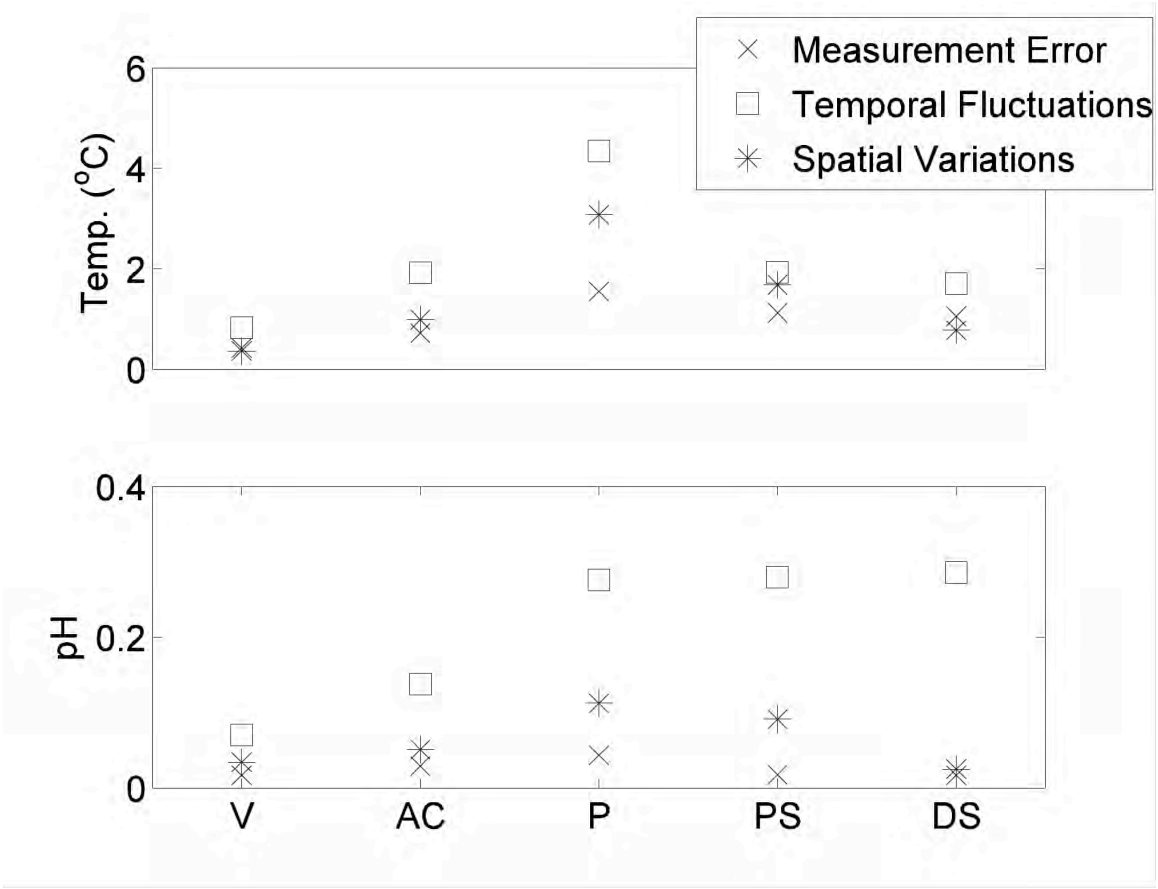

380

381 Figure 3. The three kinds of variability relevant to understanding travertine deposition
382 in comparing hot springs, organized by facies. V--vent facies. AC--apron channel.
383 P—pond. PS--proximal slope. DS--distal slope.

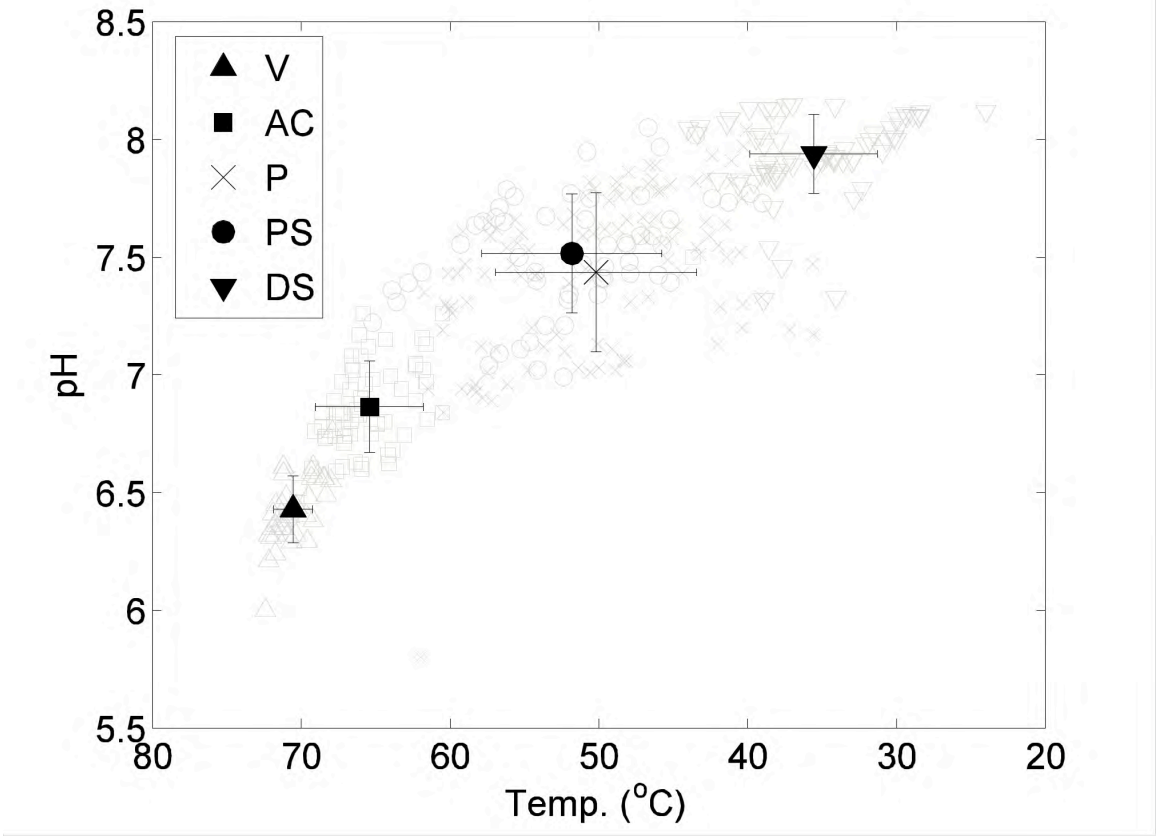

Figure 4. The distribution of 343 triplicate pH and temperature measurements taken from Springs AT-1 and AT-3 at different times. The black symbols show the facies averages, with the error bars denoting 1 standard deviation.

389 Tables

TABLE 1: Compilation of previous studies of Angel Terrace Hot Spring

Year	Spring	T/pH	Flux	Solid Chemistry	Aqueous Chemistry	Isotope Analysis	Precipitation Collection	Microbiology Samples
2005	AT-3	X	X	X	X	X	X	
2004	AT-3	X	X	X	X	X	X	X
2003	AT-3	X					X	X
2002	AT-1	X					X	X
1999	AT-1	X		X	X	X	X	X
1998	AT-1	X		X	X	X	X	X
Samples Collected	6	343	2	90	48	71	850	64

390

391 Table 1. A compilation of previous studies by our group at springs AT-1 and AT-3
392 during a 7-year period from 1998–2005. Each 'x' represents a sample or suite of
393 samples collected during field activities for each of the parameters listed at the top of
394 each column. The last row details the total number of collected samples or
395 measurements of each parameter. A triplicate measurement is reported here as a single
396 sample.

Table 2: Comparative temperature and pH ranges for each facies for previous studies

Year	Location	Value	Vent	Apron Channel	Pond	Proximal Slope	Distal Slope
2005	AT-3	T (^{o}C)	69.6	64.1	N/A	47.2	34.1
		pH	6.29	6.62		7.76	8.14
2004	AT-3	T (^{o}C)	68.0 - 72.2	60.5 – 68.6	35.6 – 61.7	50.6 – 56.4	34.2 – 39.4
		pH	6.21 – 6.57	6.59 – 7.26	6.84 – 8.04	6.99 – 7.77	7.32 – 8.07
2003	AT-3	T (^{o}C)	71.2	61.6 - 69.3	56.1 - 61.5	41.3 – 65.2	28.4 - 44.0
		pH	6.58-6.61	6.60 - 7.05	6.94 - 7.01	7.04 - 8.01	7.75 - 8.14
2002	AT-1	T (^{o}C)	67.9 - 69.3	60.5 – 64.0	59.9 – 60.3	46.7 – 50.8	24.0
		pH	6.59 – 6.76	7.00 – 7.26	7.29 - 7.30	7.95 – 8.05	8.12
1999	AT-1	T (^{o}C)	72.0 – 72.2	70.1 - 70.3	46.8 - 55.3	39.0 - 39.8	37.1 - 37.5
		pH	6.31 - 6.32	6.46 - 6.52	7.42 - 7.62	7.73 - 7.77	7.90 - 7.92
1998	AT-1	T (^{o}C)	73.2	N/A	45.3	54.2	30.2
		pH	6.00		7.43	7.40	8.00

Table 2. Temperature and pH ranges for each of the previous studies for springs AT-1 and AT-3. Studies are organized by year and facies. Temperature (^{o}C) is listed on top of pH in each row.

402 REFERENCES CITED

403 ALLEN, E.T., and DAY, A.L., 1935, Hot Springs of the Yellowstone National Park, v.
404 Publication Number 466, Carnegie Institution of Washington, 525 p.
405 AMUNDSON, R., and KELLY, E., 1987, The chemistry and mineralogy of a CO_2-rich
406 travertine depositing spring in the California Coast Range: Geochimica et
407 Cosmochimica Acta, v. 51, p. 2883-2890.
408 BARGAR, K.E., 1978, Geology and thermal history of Mammoth Hot Springs,
409 Yellowstone National Park, Wyoming, United States Geological Survey
410 Bulletin, p. 1-54.
411 BATHURST, R.G.C., 1975, Carbonate Sediments and their Diagenesis: Developments in
412 Sedimentology, v. 12: Amsterdam, Elsevier, 658 p.
413 BONHEYO, G.T., GARÇÍA MARTÍN, H., VEYSEY II, J., FRIAS-LOPEZ, J., GOLDENFELD, N.,
414 and FOUKE, B.W., 2006, Statisitcal Evaluation of Bacterial 16S rRNA Gene
415 Sequences in Relation to Travertine Mineral Precipitation and Water Chemistry
416 at Mammoth Hot Springs, Yellowstone National Park, USA: Submitted to
417 Environmental Microbiology.
418 BROCK, T.D., MADIGAN, M.T., MARTINKO, J.M., and PARKER, J., 1999, Biology of
419 Microorganisms, Prentice Hall, 991 p.
420 BUSENBERG, E., and PLUMMER, L.N., 1986, A comparative study of the dissolution and
421 crystal growth kinetics of calcite and aragonite, *in* Mumpton, F.A., ed., USGS
422 Bulletin 1578, p. 139-168.
423 CHAFETZ, H.S., and LAWERANCE, J.R., 1994, Stable isotope variability within modern
424 travertines: Geographie Physique et Quaternaire, v. 48, p. 257-273.
425 DREYBRODT, W., BUHMAN, D., MICHAELIS, J., and USDOWSKI, E., 1992, Geochemically
426 controlled calcite precipitation by CO_2 outgassing: Field measurements of
427 precipitation rates in comparison to theoretical predictions: Chemical Geology,
428 v. 97, p. 285-294.
429 FLÜGEL, E., 2004, Microfacies of Carbonate Rocks: Analysis, Interpretation, and
430 Application: Berlin, New York, Springer, 976 p.
431 FOLK, R.L., CHAFETZ, H.S., and TIEZZI, P.A., 1985, Bizarre forms of depositional and
432 diagenetic calcite in hot-spring travertines, central Italy, p. 349-369.
433 FORD, T.D., and PEDLEY, H.M., 1996, A review of tufa and travertine deposits of the
434 world: Earth-Science Reviews, v. 41, p. 117-175.
435 FOUKE, B.W., BONHEYO, G.T., SANZENBACHER, B., FRIAS-LOPEZ, J., and VEYSEY, J.,
436 2003, Partitioning of bacterial communities between travertine depositional
437 facies at Mammoth Hot Springs, Yellowstone National Park, USA: Canadian
438 Journal of Earth Science, v. 40, p. 1531-1548.
439 FOUKE, B.W., FARMER, J.D., DES MARAIS, D.J., PRATT, L., STURCHIO, N.C., BURNS,
440 P.C., and DISCIPULO, M.K., 2000, Depositional facies and aqueous-solid
441 geochemistry of travertine-depositing hot springs (Angel Terrace, Mammoth
442 Hot Springs, Yellowstone National Park, USA): Journal of Sedimentary
443 Research, v. 70, p. 265-285.

444 FOUKE, B.W., FARMER, J.D., DES MARAIS, D.J., PRATT, L., STURCHIO, N.C., BURNS,
445 P.C., and DISCIPULO, M.K., 2001, REPLY-Depositional facies and aqueous-
446 solid geochemistry of travertine-depositing hot springs (Angel Terrace,
447 Mammoth Hot Springs, Yellowstone National Park, USA): Journal of
448 Sedimentary Research, v. 71, p. 497-500.
449 FRIEDMAN, I., 1970, Some investigations of the deposition of travertine from hot
450 springs: I. The isotope chemistry of a travertine-depositing spring: Geochimica
451 et Cosmochimica Acta, v. 34, p. 1303-1315.
452 GOLDENFELD, N., CHAN, P.Y., and VEYSEY, J., 2006, Dynamics of precipitation pattern
453 formation at geothermal hot springs: Physical Review Letters, v. 96.
454 GRESSLY, A., 1838, Observations geologiques sur le Jura Solerois: Nouv. Mem. Soc.
455 Helv. Sci. Natur., v. 2, p. 1-349.
456 HERMAN, J.S., and LORAH, M.M., 1988, Calcite precipitation rates in the field:
457 Measurement and prediction for a travertine-depositing spring: Geochimica et
458 Cosmochimica Acta, v. 52, p. 2347-2355.
459 KANAKIS, J., and DALAS, E., 2000, The crystallization of vaterite on Fibrin: Journal of
460 Crystal Growth, v. 219, p. 277-282.
461 KHARAKA, Y.K., MARINER, R.H., BULLEN, T.D., KENNEDY, B.M., and STURCHIO, N.C.,
462 1991, Geochemical investigations of hydraulic connections between Corwin
463 Springs Known Geothermal Area and adjacent parts of Yellowstone National
464 Park, *in* Sorey, M., ed., Effects of Potential Geothermal Development in the
465 Corwin Springs Known Geothermal Resources Area, Montana, on the Thermal
466 Features of Yellowstone National Park, U.S. Geological Survey, p. F1-F38.
467 LIU, Z.H., and DREYBRODT, W., 1997, Dissolution kinetics of calcium carbonate
468 minerals in H_2O-CO_2 solutions in turbulent flow: The role of the diffusion
469 boundary layer and the slow reaction H_2O+CO_2 reversible arrow $H^+ + HCO_3$:
470 Geochimica Et Cosmochimica Acta, v. 61, p. 2879-2889.
471 LU, G., ZHENG, C., DONAHOE, R.J., and LYONS, W.B., 2000, Controlling processes in a
472 $CaCO_3$ precipitating stream in Huanlong Natural Science District, Sichuan,
473 China: Journal of Hydrology, v. 230, p. 34-54.
474 PENTECOST, A., 1990, The formation of travertine shrubs: Mammoth Hot Springs,
475 Wyoming: Geological Magazine, v. 127, p. 159-168.
476 READING, H.G., 1996, Sedimentary Environments: processes, Facies and Stratigraphy:
477 London, England, Blackwell Science Ltd., 688 p.
478 SOREY, M.L., 1991, Effects of potential geothermal development in the Corwin Springs
479 known geothermal resources area, Montana, on the thermal features of
480 Yellowstone National Park: Menlo Park, CA, United States Geological Survey.
481 SPANOS, N., and KOUTSOUKOS, P.G., 1998, Kinetics of Precipitation of Calcium
482 Carbonate in Alkaline pH at Constant Supersaturarion. Spontaneous and Seeded
483 Growth: Journal of Physical Chemistry, v. 102, p. 6679-6684.
484 STURCHIO, N.C., MURRELL, M.T., PIERCE, K.L., and SOREY, M.L., 1992, Yellowstone
485 Travertines: U-series Ages and Isotope Ratios (C, O, Sr, U), *in* Kharaka, and
486 Maest, eds., Water-Rock Interaction: Rotterdam, Balkema, p. 1427-1430.

487 STURCHIO, N.C., PIERCE, K.L., MURRELL, M.T., and SOREY, M.L., 1994, Uranium-
488 series ages of travertines and timing of the last glaciation in the northern
489 Yellowstone area, Wyoming-Montana: Quaternary Research, v. 41, p. 265-277.
490 SUAREZ, D.L., 1983, Determination of calcite precipitation rates in irrigated arid land
491 soils: Abstracts with Programs - Geological Society of America, v. 15, p. 701.
492 USDOWSKI, E., HOEFS, J., and MENSCHEL, G., 1979, Relationship between $\delta^{13}C$ and
493 $\delta^{18}O$ fractionation and changes in major element composition in a recent calcite-
494 depositing spring - a model of chemical variations with inorganic $CaCO_3$
495 precipitation: Earth and Planetary Science Letters, v. 42, p. 267-276.
496 VAN CAPPELLEN, P., CHARLET, L., STUMM, W., and WERSIN, P., 1993, A Surface
497 Complexation Model of the Carbonate Mineral-Aqueous Solution Interface:
498 Geochimica Et Cosmochimica Acta, v. 57, p. 3505-3518.
499 WALKER, R.G., 1984, Facies Models: St. Johns, Newfoundland, Geological Association
500 of Canada, 317 p.
501 WHITE, D.E., FOURNIER, R.O., MUFFLER, L.P.J., and TRUESDELL, A.H., 1975, Physical
502 results of research drilling in thermal areas of Yellowstone National Park,
503 Wyoming: Menlo Park, California, United States Geological Survey.
504 WILSON, J.L., 1975, Carbonate Facies in Geologic History: New York, Springer-Verlag,
505 472 p.
506 ZHANG, D.D., ZHANG, Y.J., ZHU, A., and CHENG, X., 2001, Physical mechanisms of
507 river waterfall tufa (travertine) formation: Journal of Sedimentary Research, v.
508 71, p. 205-216.
509